2018 26th Mediterranean Conference on Control and Automation (MED)
Zadar, Croatia, June 19-22, 2018

Energy-Efficient Train Traction Control on Complex Rail Configurations

Hrvoje Novak* and Mario Vašak†
University of Zagreb, Faculty of Electrical Engineering and Computing
Laboratory for Renewable Energy Systems (url: www.lares.fer.hr)
*hrvoje.novak@fer.hr, †mario.vasak@fer.hr

***Abstract*— In the presented work, control system for energy-efficient train operation with inclusion of a detailed train motion model and a varying rail path configuration is developed. Piecewise affine train model is constructed with the parameters obtained for the electromotive train manufactured by Croatian train producer company Končar - Electric Vehicles Inc. The model encompasses intrinsic features of the train system such as linearized resistance force, various traction and braking force limitations and passengers comfort constraints. Curves and slopes are introduced as rail path segments with different resistance forces and incorporated in the optimization procedure. The resulting quadratic optimization problem is solved parametrically through dynamic programming with the off-line precomputed optimal control law obtained as a function of train speed and traversed path. Control system is evaluated on a simulation scenario with Končar's electromotive train and a rail path configuration with a varying slope.**

***Index Terms*— energy-efficient train traction control, piecewise affine train model, multiparametric quadratic programming, complex rail path configuration**

I. INTRODUCTION

With the rising of global demand for transport [1], the ability to meet the transport demands in a sustainable way becomes increasingly important. Due to capacity, safety and reliability, railway transport systems play an important role in the overall transport sector, however still consuming large quantities of energy in day to day operation [2]. With almost over 50% of the overall energy of railway transport systems being consumed by trains in urban rail transit [3] reducing the trains tractive energy consumption has been in a lot of focus during the past few decades.

The focus of this work is put on increasing the energy efficiency of the railway transport system through optimization of the trains driving profile, i.e. minimization of the on-route energy consumption of each individual train while respecting the timetables, on-route restrictions (speed limits, train traction force boundaries) and passengers comfort. Research on energy-efficient train driving can be summed into analytical and numerical optimization methods [4], [5]. Initially developed optimization methods were based on analytical principles such as Pontryagin's maximum principle as used in [6], [7] or [8] and result in an optimal train trajectory divided in 4 different segments: (i) maximum acceleration, (ii) cruising at constant speed, (iii) coasting and (iv) maximum deceleration. Numerical optimization algorithms came into focus during the recent years, with the steady increase in available computing power and efficiency of optimization algorithms [5]. Examples of numerical algorithms used for energy-efficient train control are based on fuzzy logic as in [9], genetic algorithms in [10] or various dynamic programming approaches such as [11]. Analytical methods require good objective function properties and hardly cope with more realistic conditions that introduce complex nonlinear terms into the optimization, while on the other hand, numerical methods suffer from long computation times and cannot guarantee the optimality of the obtained solution. Therefore a trade-off between accuracy and computational efficiency is often suggested [4], [5].

Energy-efficient train control problem with a simple train model has been formulated and solved in [12]. The optimal train control law is calculated by utilizing the multiparametric quadratic programming resulting in a time-varying piecewise affine function, which relates the traction force to the train position and speed. Therefore, the control law is computed off-line and can be easily evaluated on-line. However, in the considered train model, maximum traction/braking force is available during all train speeds and the considered rail path is without curves and slopes. In the presented work an extension of the piecewise affine (PWA) train model from [12] is presented with the main goal of covering all relevant train characteristics thus making the proposed control system from [12] more realistic: (i) discrete time piecewise affine (DTPWA) train model is detailed with introduction of additional resistance force parameters and traction/braking force limitations for different train speeds, (ii) rail path configuration is extended through inclusion of slopes and curves to the path configuration in the form of additional DTPWA train models and (iii) simulation scenarios are performed with train composition parameters obtained from Končar - Electric Vehicles Inc., a Croatian train producer company, thus bringing the obtained results closer to those achievable in actual industrial applications.

The paper is structured as follows. In Section II mathematical model of the train motion is described together with resistance force parameters for various rail path configurations and traction/braking force constraints. In Section III the construction procedure of the DTPWA train model is presented. Energy-efficient train control algorithm is described in Section IV. Simulation scenario parameters and results are presented in Section V with final conclusions given in Section VI.

978-1-5386-7891-6/18/$31.00 ©2018 IEEE

II. MATHEMATICAL MODEL

Train motion along the rail path can be described with a simple continuous-time model [12]:

$$m\rho\frac{dv}{dt} = F(t) - F_r(v,s), \tag{1a}$$

$$\frac{ds}{dt} = v, \tag{1b}$$

where m is the train mass, ρ is the rotating mass factor (takes into account the rotational energy of the trains rotating parts as an addition to the overall train mass m), v is the train velocity, s the traversed path of the train, F the train traction force (negative for braking force), and F_r is the overall resistance force to the train movement along the tracks.

A. Resistance force components

The overall resistance force F_r can be divided into [4]:

$$F_r(v,s) = F_{rb}(v) + F_{rl}(v,s), \tag{2}$$

where $F_{rb}(v)$ is the basic resistance which includes friction (roll resistance) and aerodynamic resistance, and $F_{rl}(v,s)$ is the line resistance which is caused by different rail path configurations, namely track grade, curves and tunnels [4].

The basic resistance $F_{rb}(v)$ can then be described according to the Strahl formula [13]:

$$F_{rb}(v) = k_1 + k_2 v + k_3 v^2, \tag{3}$$

with k_1, k_2 and k_3 being coefficients determined from the actual train shape, its power train and wind speed, and can be calculated from the data known about the train.

Line resistance F_{rl} depends on the actual rail path that the train is currently traveling on and can be described with the following expression [14]:

$$F_{rl}(v,s) = mg\sin(\alpha(s)) + f_c(r(s)) + f_t(v, l_t(s)), \tag{4}$$

where g is the gravitational constant, $\alpha(s)$ the slope of the rail tracks and $r(s)$ the curve radius. First term accounts for the track grade resistance and represents the gravity force component that is parallel with the slope of the track.

Curve resistance f_c is a consequence of the rigid axle-wheels connection and the centrifugal force. Because of the rigid connection, inner and outer wheels have the same angular velocity but have a different track length along the curve and therefore cause additional friction as a resistance to train movement. Curve resistance can be calculated with Roeckl's empirical formula [15]:

$$f_c(r(s)) = \frac{6.3}{r(s) - 55} \text{ Nm} \quad for \quad r(s) \geq 300 \text{ m}, \tag{5a}$$

$$f_c(r(s)) = \frac{4.91}{r(s) - 30} \text{ Nm} \quad for \quad r(s) < 300 \text{ m}. \tag{5b}$$

Tunnel resistance f_t is a consequence of higher aerodynamic resistance in the tunnel determined by the tunnel form, smoothness of tunnel walls, exterior surface of the train etc. and is often described with empirical expressions. It can be described, depending on the existence of a limiting gradient [4], as:

$$f_t(v, l_t(s)) = 1.296 \cdot 10^{-9} l_t(s) mg v^2, \tag{6a}$$

or if all track gradients can be climbed without the help of a second power unit:

$$f_t(v, l_t(s)) = 1.3 \cdot 10^{-7} l_t(s) mg, \tag{6b}$$

where $l_t(s)$ is the tunnel length. Tunnel resistance is not considered in the paper since tunnels are rarely required in city and inter-city rail traffic. However, it can be included in the train model by implementing the same procedure as for curves or track gradients.

B. Available traction/braking force

Train traction force F is bounded by the maximum traction force F_{max} which is a function of the trains velocity v. At low speeds, maximum traction force is bounded by the adhesion limit, while at higher speeds it is bounded by the characteristics of the powertrain which determines the maximum tractive power and the maximum train speed.

Adhesion is defined as the ratio of the longitudinal force actually applied at the wheel/rail contact (in this case tractive effort) to the vertical reaction force (instantaneous axle load on powered wheelsets), and can be considered equal to the coefficient of friction between wheel and rail at its limiting value. Due to adhesion, the maximum traction force that can be transferred on to the tracks can be calculated as:

$$F_{\max} = \mu(v) m_a g \cos(\alpha(s)), \tag{7}$$

where $\mu(v)$ is the adhesion coefficient and m_a the adhesion mass. Adhesion coefficient can then be calculated with the following empirical expression [16]:

$$\mu(v) = 0.161 + \frac{7.5}{v + 44}. \tag{8}$$

Additionally, in order to ensure the passenger's comfort, train acceleration is usually limited to 1.1 m/s^2, resulting with different limitations to the traction force, depending on the trains mass and the rail path configuration.

III. DISCRETE TIME PIECEWISE AFFINE TRAIN MODEL

A. Končar electromotive train

Train composition model is based on the low-floor electromotive train manufactured by Končar - Electric Vehicles Inc. The considered electromotive train (EMT) is intended for urban and commuter operation and designed as low floor four-part train with the total length of 75 m (construction scheme depicted in Fig. 1), and was built for rails electrified with catenary power supply of 25 kV voltage and 50 Hz frequency.

Three-phase asynchronous traction motors provide high acceleration at start-up and a maximum speed of 160 km/h. Train braking system is designed as a combination of regenerative and pneumatic frictional brakes, which together, provide the necessary braking force (pneumatic frictional

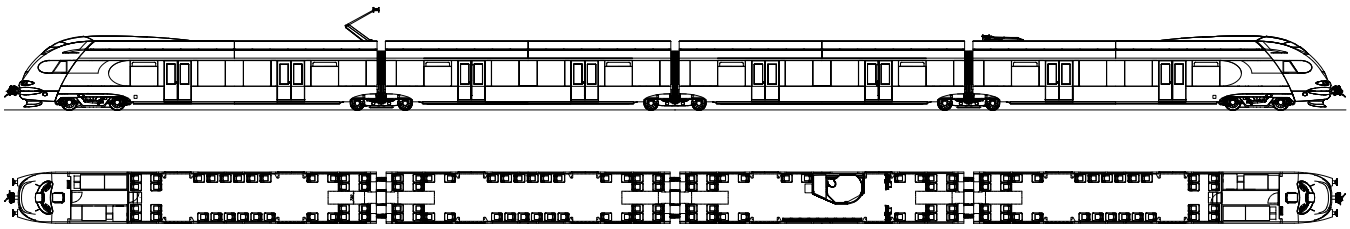

Fig. 1. Construction scheme of Končar - Electric Vehicles electromotive train for urban and commuter operation [17].

braking is utilized in lower speeds when regenerative braking is not able to provide enough braking force to stop the train) [17], [18]. Parameters of the EMT are obtained from Končar - Electric Vehicles Inc. and presented in Table I together with resistance and traction effort curves in Fig. 2 and Fig. 3, respectively. Resistance curve parameters are obtained for a train mass of 172 t and a straight rail path with no gradient.

TABLE I

KONČAR ELECTROMOTIVE TRAIN PARAMETERS

Parameter	Value
Catenary supply voltage	25 [kV], 50 [Hz]
Composition weight	139 [t]
Max. weight	172 [t]
Overall length	75 [m]
Gauge	1435 [mm]
Powered boogie axle/wheel radius	180/750 [mm]
Trailer boogie axle/wheel radius	180/860 [mm]
Seating capacity	up to 220
Standing capacity	up to 300 (4 pers./m^2)
Continuous power (on wheel)	2000 [kW]
Starting traction force	200 [kN]
Max. acceleration at gross weight:	> 1 [m/s^2]
Max. deceleration	> 1.3 [m/s^2]
Max. velocity	44.44 [m/s]
Specific resistance force	$856 + 36v + 5.4432v^2$ [N]
Adhesion mass	70 [t]
Rotating mass factor	1.05
Motor-reductor efficiency	0.939
Converter efficiency	0.95

B. Resistance force linearization

Continuous-time model from (1a) is nonlinear due to the aerodynamic resistance in (3). The nonlinearity (3) is approximated with two straight lines around $v_0 = 22.22$ m/s and separate dynamics are created for both affine segments of the linearized resistance force [12]:

$$\dot{x} = \begin{cases} A_1 x + B_1 u + a_1 & \text{if} \quad v \le v_0, \\ A_2 x + B_2 u + a_2 & \text{if} \quad v \ge v_0, \end{cases} \tag{9}$$

where $x = \begin{bmatrix} v \\ s \end{bmatrix}$, $u = F$, $A_i = \begin{bmatrix} -\frac{a_i}{m} & 0 \\ 1 & 0 \end{bmatrix}$, $B_i = \begin{bmatrix} \frac{1}{m} \\ 0 \end{bmatrix}$, $a_i = \begin{bmatrix} -\frac{b_i}{m} \\ 0 \end{bmatrix}$.

After Zero-Order Hold (ZOH) discretization of the PWA model with sampling time $T = 15$ s is performed. Sample time of 15 s is chosen as a compromise between capturing of relevant train dynamics as well as ensuring the linearization accuracy and the numerical efficiency of the optimization algorithm. Discretization results in the following DTPWA model:

$$x_{k+1} = f_{\text{PWA}}(x_k, u_k), \tag{10}$$

where:

$$\begin{aligned} f_{\text{PWA}}(x_k, u_k) &= A_{di} x_k + B_{di} u_k + a_{di}, \\ \text{if} \quad H_i x_k + L_i u_k &\le K_i, \quad i = 1,2,3,4, \end{aligned} \tag{11}$$

with matrices H_i, L_i and K_i formed according to constraints for each DTPWA dynamics. Since simple discretization of both affine dynamics using zero-order hold and comprising them into a DTPWA model could lead to faulty behavior when crossing speed v_0 between two sampling instants, transitional dynamics, described with matrices A_{d3}, B_{d3} and vector a_{d3}, are introduced into (10) for both transitional dynamics, resulting in the following piecewise affine (PWA) model:

$$x_{k+1} = \begin{cases} A_{d1} x_k + B_{d1} u_k + a_{d1} \\ \quad \text{if} \quad v_k \le v_0, \ v_{k+1} \le v_0, \\ A_{d2} x_k + B_{d2} u_k + a_{d2} \\ \quad \text{if} \quad v_k \ge v_0, \ v_{k+1} \ge v_0, \\ A_{d3} x_k + B_{d3} u_k + a_{d3} \\ \quad \text{if} \quad v_k \le v_0, \ v_{k+1} \ge v_0, \\ A_{d3} x_k + B_{d3} u_k + a_{d3} \\ \quad \text{if} \quad v_k \ge v_0, \ v_{k+1} \le v_0. \end{cases} \tag{12}$$

Mechanical energy required for the train within one sampling interval $I = [kT, (k+1)T)$ is:

$$\begin{aligned} E_I(F(kT), v(kT)) &= \int_{kT}^{(k+1)T} F(kT) v(\tau) d\tau = \\ &= p_i (F(kT))^2 + q_i F(kT) + r_i F(kT) v(kT), \end{aligned} \tag{13}$$

where $p_i = \frac{1}{a_i}\left[T - T_i\left(1 - e^{-\frac{T}{T_i}}\right)\right]$, $q_i = -b_i p_i$, $r_i = T_i\left(1 - e^{-\frac{T}{T_i}}\right)$, the index i represents the currently activated dynamics. It is important to mention that $p_i > 0$ if $a_i > 0$ which leads to convex energy optimization problems with respect to the traction force [12].

Transition line $a_3 v + b_3$ is introduced to penalize its use in the sense of consumed energy since otherwise the discrete-time nature of the linearized model would be used by the optimal controller to virtually decrease the force resistance by permanently performing transitions around v_0. Results of the resistance force linearization are depicted in Fig. 2 with the parameters of Končar's electromotive train.

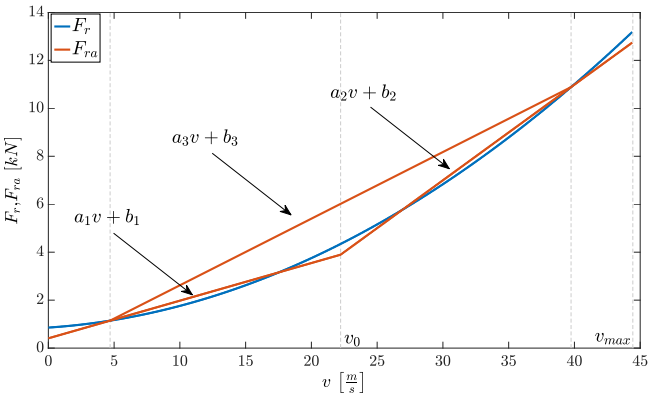

Fig. 2. Linearized model F_{ra} of Končar's electromotive train resistance force F_r for the parameters from Table I.

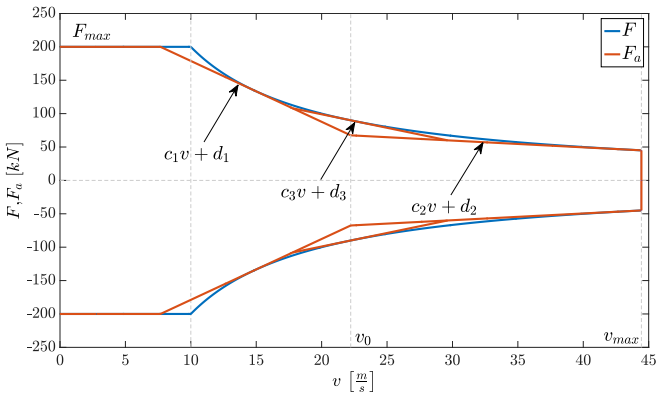

Fig. 3. Linearized model F_a of the available traction and braking force limits F for the parameters of Končar's electromotive train from Table I.

C. Traction/braking force constraints

Available traction and breaking forces are highly dependent on the current train speed v and are described with the trains tractive effort curve. Tractive effort curve data have been obtained from Končar and linearized. The obtained constraints $c_iv_k+d_i$ are subsequently added to the DTPWA train model as:

$$\begin{aligned} F_k &\leq c_iv_k+d_i, \qquad i=1,2,3,\\ F_k &\geq -c_iv_k-d_i, \qquad i=1,2,3, \end{aligned} \tag{14}$$

where c_i and d_i are coefficients obtained from linearization of the tractive effort curve and i corresponds to each of the dynamics from (12). The linearization is depicted in Fig. 3, where it is shown that both traction and breaking force have been under-approximated to compensate for the linearization error and ensure that the train has the available force to safely and punctually arrive at the station.

Due to the discretization of the train model, it is possible that during the discretization interval k, lasting 15 seconds, the trains speed changes significantly thus allowing the controller to use the amount of traction force which is not available in realistic implementations. Therefore constraints are added limiting the available traction/braking force with respect to the current speed v_k as well as the speed in the next discretization step v_{k+1}:

$$\begin{aligned} F_k &\leq c_i\frac{v_k+v_{k+1}}{2}+d_i, \qquad i=1,2,3,\\ F_k &\geq -c_i\frac{v_k+v_{k+1}}{2}-d_i, \qquad i=1,2,3. \end{aligned} \tag{15}$$

Passengers comfort is ensured through addition of the acceleration limit $a_{\max} \leq 1.3$ m/s^2 such that heavy acceleration or deceleration periods are avoided. The limit is introduced through addition of the following bounds to the traction force F in each dynamics i:

$$-a_{\max} \leq \frac{1}{m}(F-a_iv-b_i) \leq a_{\max}. \tag{16}$$

D. Curves and slopes introduction

Different rail path configurations such as curves and slopes, as a consequence result in a different overall resistance force $F_r(v,s)$ from (2). For each track segment j a separate DTPWA train model is created, with the above-described procedure and the models now being separated not only by train speed v, but also by the traversed path s in the rail path points that separate two adjacent segments. Again, simple merging of such models would result in faulty controller behavior where track segments with lower resistance force are preferred.

Therefore, transition affine models are introduced for time intervals where the transition between two adjacent path segments with different slopes or curves occurs, i.e. $s_k \leq s_t$ and $s_{k+1} \geq s_t$, with s_t marking the rail path point between two adjacent path segments. With the resistance force in one track segment being $F_{r,j}$ and in the following adjacent track segment $F_{r,j+1}$ (calculated from the expression in (2)), the resistance force $F_{r,j,j+1}$ used for creation of the transition affine models is simply described with:

$$F_{r,j,j+1} = F_{rb,j+1} + \frac{F_{rl,j}+F_{rl,j+1}}{2}. \tag{17}$$

Through introduction of such crossing models, a compromise is achieved between the controller avoiding the higher resistance track segments (e.g. during train travels from a flat segment to an ascent where the controller has the tendency to stay in the rail segment with lower resistance force as long as possible) and not utilizing the accumulated kinetic energy in lower resistance track segments if the affine models for different track segments were strictly separated (e.g. when descending to a flat rail segment where the controller would lose the possibility to exploit the trains inertia obtained from the descent). Another important argument is that the transition from one slope to the other is usually gradual on actual profiles, and this approach practically averages the two slopes on the transition and thus makes the transition gradual.

Although not considered in this paper, introduction of tunnel resistance is straightforward. Calculated tunnel resistance $f_t(v,l_t(s))$ from (6) is added to the overall resistance force $F_r(v,s)$ from (2) which is linearized by the same procedure described above, for a tunneled segment.

IV. ENERGY-EFFICIENT TRAIN DRIVING CONTROL PROBLEM

Energy-efficient optimal train control problem (depicted in Fig. 4) is stated as follows: at the current time, denoted with $t=0$ and characterized with known train velocity v_0 and train position on the rail track s_0, find the optimal train traction and braking force profile that minimizes the trains mechanical energy consumption, while reaching the next station at time $t=T^*$ and respecting all given constraints on v, s and F along the rail path [12]:

$$\min_{F} \quad E=\int_0^{T^*} F(t)v(t)dt, \tag{18}$$

subject to train dynamics described in (1a), constraints:

$$\begin{aligned} f(v(t),F(t)) &\leq 0, \\ 0 \leq v(t) &\leq V_{\max}(s), \end{aligned} \tag{19}$$

and boundary conditions:

$$\begin{aligned} s_0 &= s_{\text{start}}, & v_0 &= v_{\text{start}}, \\ s(T^*) &= s_{\text{end}}, & v(T^*) &= v_{\text{end}}, \end{aligned} \tag{20}$$

where $V_{\max}(s)$ is the maximum allowed velocity (depends on train characteristics and the current track section limitations), $f(v,F)\leq 0$ describes the space of attainable points in speed-force plane of the train, s_{start} and v_{start} are train position and velocity at the start of the route and s_{end} and v_{end} are train position and velocity at the end of the route. Duration of the trip T^* between s_{start} and s_{end} is usually provided by the railway system operator through timetables.

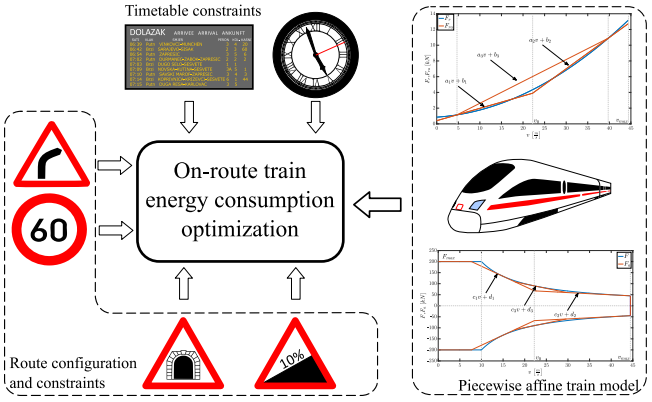

Fig. 4. Energy-efficient train driving optimization problem scheme.

In [12] the control problem formulated in (18)-(20) is solved by using the DTPWA model (10)-(13) backwards in time with dynamic programming through $k^*=T^*/T$ steps:

$$J_k(x_k,u_k) = E_I(x_k,u_k)+J^*_{k+1}(x_{k+1}), \tag{21}$$

$$J^*_k(x_k) = \min_{u_k} J_k(x_k,u_k), \tag{22}$$

$$s.t. \quad f_{\text{PWA}}(x_k,u_k)\in \mathscr{X}^{k+1}, \tag{23}$$

$$h(x_k,u_k)\leq 0, \tag{24}$$

where $k=k^*-1,k^*-2,\ldots,0$, h is a vector of constraints on x_k and u_k incorporating the maximal allowable and possible train traction and braking force F_{max} and speed V_{max}, E_I is described by (13),

$$\mathscr{X}^k=\left\{x|\exists u: f_{\text{PWA}}(x,u)\in \mathscr{X}^{k+1}, h(x,u)\leq 0\right\}, \tag{25}$$

and terminal conditions are:

$$\begin{aligned} \mathscr{X}^{k^*} &= \begin{bmatrix} 0 \\ s_{\text{end}} \end{bmatrix}, \\ J^*_{k^*} &= 0. \end{aligned} \tag{26}$$

Minimization procedure from (21)-(26) is performed off-line resulting in an optimal control law $u^*_k(x_k)$ in a PWA form. The off-line computed u^*_k and J^*_k are represented with N_k polytopes, their corresponding affine control law u_k and quadratic cost J_k are easily evaluated during on-line train operation where only the traversed path s and train speed v are required as current train state information [12].

V. SIMULATION RESULTS

Data considered for evaluation of the energy-efficient train control system is based on the DTPWA train model with Končar's electromotive train parameters from Table I and a rail path with parameters presented in Table II. Rail path configuration used for simulation consists of two separate segments with equal lengths of 3 kilometers. First segment of the rail path is straight with no gradient while the second segment is straight but with track incline of 1.5°. Train travel was simulated for designated travel times T^* set to 5 and 10 minutes, all with a time step of $T=15$ s.

TABLE II
RAIL PATH PARAMETERS

Rail path segment	Length [km]	Track description
1	3	Straight tracks with no track gradient
2	3	Straight tracks with 1.5° track incline

In Figures 5 and 6 optimal train traction force profiles F^* with corresponding train speeds $\bar{v}$ and traversed paths $\bar{s}$ are presented for travel times of 5 and 10 minutes, respectively.

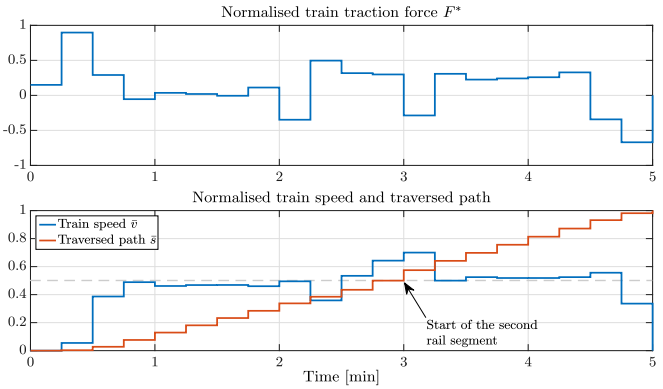

Fig. 5. Energy-efficient train traction force profile F^*, train speed $\bar{v}$ and traversed path $\bar{s}$ for travel time of 5 minutes.

For train travel duration of 10 minutes the train consumed 137.9 MJ of energy, while for the shorter travel time of

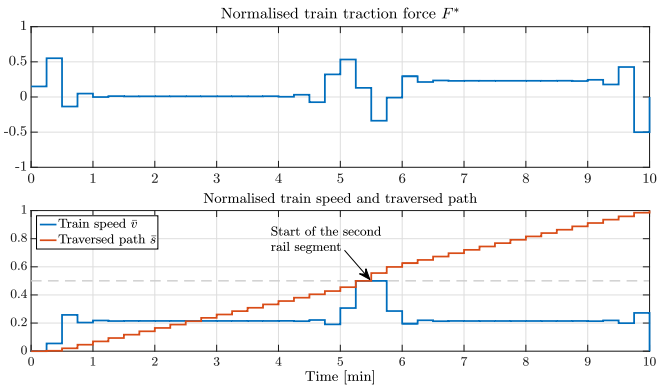

Fig. 6. Energy-efficient train traction force profile F^*, train speed $\bar{v}$ and traversed path $\bar{s}$ for travel time of 10 minutes.

5 minutes the overall consumed energy was 149.3 MJ. As expected, shorter travel time resulted in more overall energy consumed since the train is required to accelerate more rapidly in order to reach the station in time. Optimal energy costs for travel duration of 10 minutes are presented in Fig. 7 with respect to the initial train speed and starting position on the route. It is shown that, depending on the starting speed and position on the route, train consumes a larger amount of energy to reach the destination in allotted travel time of 10 minutes.

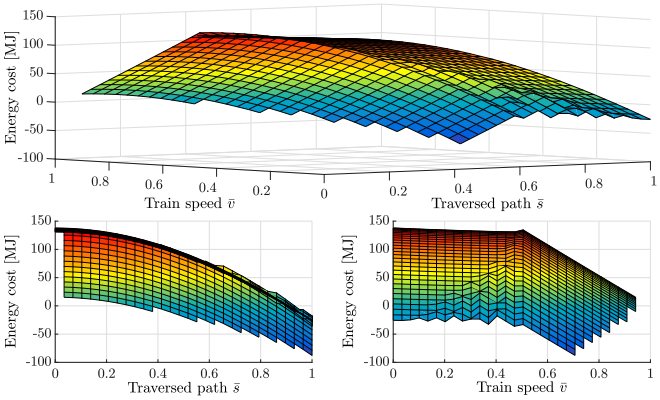

Fig. 7. Optimal energy costs J^* with respect to initial train speed and traversed path on the route for travel time of 10 minutes.

VI. CONCLUSION

Energy-efficient train control system with a detailed train model is presented in the paper. Train model includes various traction/braking force limitations and a linearized resistance force model with data based on train composition parameters obtained from the Croatian train producer company Končar. Rail path configuration with a varying slope is modeled and used for verification on the developed control system. Multi-parametric quadratic programming was used to calculate the optimal train control law resulting in a time-varying piecewise affine function, relating the traction force to the train position and speed thus making the off-line computed control law easily evaluated on-line during real-time train operation.

ACKNOWLEDGMENT

This work has been fully supported by Croatian Science Foundation under the project No. 6731 (project 3CON – Control-based Hierarchical Consolidation of Large Consumers for Integration in Smart Grids, http://www.fer.unizg.hr/3con) and by the Danube Transnational Programme through the project Smart Building - Smart Grid - Smart City (3Smart, http://www.interreg-danube.eu/3smart), grant DTP1-502-3.2-3Smart. The authors are grateful to Končar - Electric Vehicles Inc. for their contributions and provided electromotive train parameters. This research has also been carried out within the activities of the Centre of Research Excellence for Data Science and Cooperative Systems supported by the Ministry of Science and Education of the Republic of Croatia.

REFERENCES

[1] "European Commission. EU Transport in figures: Statistical pocketbook 2014." [Online]. Available: http://ec.europa.eu/transport/facts-fundings/statistics/doc/2014/pocketbook2014.pdf

[2] International Energy Agency and International Union of Railways, "Railway Handbook 2017 - Energy Consumption and CO_2 Emissions."

[3] A. González-Gil, R. Palacin, P. Batty, and J. Powell, "A systems approach to reduce urban rail energy consumption," *Energy Conversion and Management*, vol. 80, 04 2014.

[4] Y. Wang, B. Ning, T. van den Boom, and B. de Schutter, *Optimal Trajectory Planning and Train Scheduling for Urban Rail Transit Systems*, ser. Advances in Industrial Control. Springer International Publishing, 2016.

[5] X. Yang, X. Li, B. Ning, and T. Tang, "A survey on energy-efficient train operation for urban rail transit," *IEEE Transactions on Intelligent Transportation Systems*, vol. 17, no. 1, pp. 2–13, Jan 2016.

[6] P. G. Howlett and P. J. Pudney, *Energy-Efficient Train Control*, ser. Advances in Industrial Control. Springer London, 1995.

[7] P. Howlett, "The optimal control of a train," *Annals of Operations Research*, vol. 98, no. 1, pp. 65–87, Dec 2000.

[8] I. M. Golovitcher, "Energy efficient control of rail vehicles," in *2001 IEEE International Conference on Systems, Man and Cybernetics*, vol. 1, 2001, pp. 658–663 vol.1.

[9] C. S. Chang and D. Y. Xu, "Differential evolution based tuning of fuzzy automatic train operation for mass rapid transit system," *IEE Proceedings - Electric Power Applications*, vol. 147, no. 3, pp. 206–212, May 2000.

[10] C. S. Chang and S. S. Sim, "Optimising train movements through coast control using genetic algorithms," *IEE Proceedings - Electric Power Applications*, vol. 144, no. 1, pp. 65–73, Jan 1997.

[11] M. Miyatake and H. Ko, "Optimization of train speed profile for minimum energy consumption," *IEEJ Transactions on Electrical and Electronic Engineering*, vol. 5, no. 3, pp. 263–269, 2010.

[12] M. Vašak, M. Baotić, N. Perić, and M. Bago, "Optimal rail route energy management under constraints and fixed arrival time," in *Proceedings of the European Control Conference*, 2009, pp. 2972–2977.

[13] B. Rochard and F. Schmid, "A review of methods to measure and calculate train resistances," *Proceedings of the Institution of Mechanical Engineers, Part F: Journal of Rail and Rapid Transit*, vol. 214, no. 4, pp. 185–199, April 2000.

[14] B. Mao, "The calculation and design of train operation," Beijing, China: People Transport press, 2008.

[15] A. Nash and D. Huerlimann, "Opentrack-simulation of railway networks, user manual version 1.3," *Institute for Transportation Planning and Systems. ETH Zurich. Switzerland*, 2003.

[16] E. W. Curtius and A. Kniffler, "Neue erkenntnisse über die haftung zwischen treibrad und schienen," *Elektrische Bahnen*, vol. 21, no. 9, pp. 201–210, 1950.

[17] Končar Electric Vehicles Inc., "Low-floor Electric Multiple Unit for Urban and Commuter Operation," http://www.koncar-kev.hr/docs/koncarkevEN/documents/19/2_1/Original.pdf.

[18] Končar Electric Vehicles Inc., "Electric Multiple Units," http://www.koncar-kev.hr/products_and_services/electric_multiple_units.